PYROCLASTIC DEPOSITS WITHIN FLOOR-FRACTURED MERSENIUS CRATER. J.Olaf Gustafson[1], L.R. Gaddis[2], B.R. Hawke[3], and T.A. Giguere[3,4]. [1]Dept. Earth & Atmospheric Sciences, Cornell University, Ithaca, NY; [2]Astrogeology Science Center, U.S. Geological Survey, Flagstaff, AZ; [3]Hawaii Institute of Geophysics and Planetology, University of Hawaii, Honolulu, HI; [4]Intergraph Corporation, Kapolei, HI. (jg72@cornell.edu).

Introduction: Numerous localized pyroclastic deposits have been identified within the Nectarian floor-fractured crater Mersenius (D= 84 km), located in the highlands west of Mare Humorum (21.5°S, 49.2°W) [1-3]. Recent data from the camera subsystems aboard the Lunar Reconnaissance Orbiter (LRO) and SELENE/Kaguya spacecraft [4-6] enable more detailed analysis of these pyroclastic deposits. We are using high-resolution monochrome data from the LRO Narrow Angle Camera (NAC; resolution ~0.5-2.0 m/pixel) to examine deposit morphologies, surface textures, and potential source vents. We are also using multispectral data from the LRO Wide Angle Camera (WAC; two ultraviolet (UV) and five visible (VIS) wavelengths from 320-690 nm; resolution ~400 m/px in the UV and ~75 m/px in the visible) and the Kaguya Multiband Imager (MI; five VIS and near-infrared (NIR) wavelengths from 415-1000 nm; resolution ~20 m/px) to constrain deposit compositions and look for differences in mineralogy and/or glass content between deposits. We also use derived products from these data sets including the WAC GLD100 DTM [7] and Kaguya MI FeO and TiO_2 abundances [8].

Background: Lunar pyroclastic deposits (LPDs) have been identified across the Moon, often on the basis of their low albedo, smooth texture, and mantling effect over underlying terrain features [9,10,11]. The composition and distribution of these materials provide important clues to the history of lunar volcanism and the composition of the interior. Analysis of pyroclastic glass samples has indicated that many are enriched in metallic and volatile elements (e.g. Fe, Ti, Zn, S), and they are of interest both as samples of the lunar interior and as potential targets for resource extraction [12,13,14]. Deposits of both regional (roughly >1000 km^2) and localized (tens to hundreds of km^2) extent have been documented; localized deposits are often associated with endogenic craters or depressions [10,15].

Effusive and pyroclastic volcanic deposits north and west of Mare Humorum have been described by others (e.g. 1-3,16). Mersenius was identified as a Class 3 floor-fractured crater following the classification system of Schultz (1976)[17]. Such craters are thought to have been modified by intrusion of magma beneath the crater floor [17,18]. Several small pyroclastic deposits have identified on the floor of Mersenius [1]. Previous studies using Clementine data found that two of the deposits have a basaltic composition [2].

Results and Discussion: MI and WAC color images of Mersenius clearly delineate the four deposits previously identified by Hawke & Coombs (Figs. 2&3). The "NW" deposit is resolved into two distinct deposits, and a possible 6th deposit is visible to the east (labeled "NE" in Fig. 3). All six deposits align with the concentric rille/fracture system at the edge of the crater floor. Relative TiO_2 abundances derived from the MI data show a clear enhancement associated with all six deposits (Fig. 4); this provides additional evidence that the NE deposit is an additional pyroclastic deposit related to the other five. Its subdued appearance is probably due to a partial covering of ejecta from the ~6 km crater directly east of the deposit..

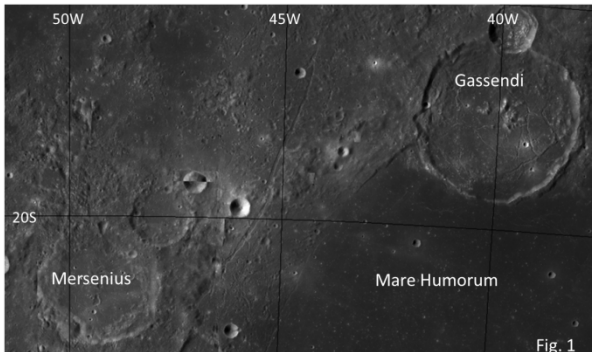

Fig. 1 - Mersenius crater (D= 84 km) is located west of Mare Humorum (portion of global WAC mosaic; NASA/GSFC/ASU)

A WAC GLD100 topographic profile through the northern deposits (WNW and NW (a&b), Fig. 5) reveals that the endogenic source craters associated with these deposits are 6-8 km wide and up to 300 m deep. A NAC image of the NW source crater is shown in Fig. 6. No clear vent is seen in the crater, likely because of infilling from mass wasting and numerous superposed impact craters.

Conclusions and Future Work: The use of the LROC WAC, NAC, and Kaguya MI data sets for analysis of the Mersenius localized pyroclastic deposits is enabling more detailed characterization of the extent, morphology, and composition of these materials. Future work will include more detailed analysis of possible source craters and development of quantitative estimates of FeO and TiO_2 abundance with the goal of better understanding the relationship between the Mersenius deposits and other nearby volcanic units, including those in Gassendi crater and the Mare Humorum mare basalts.

Fig. 2

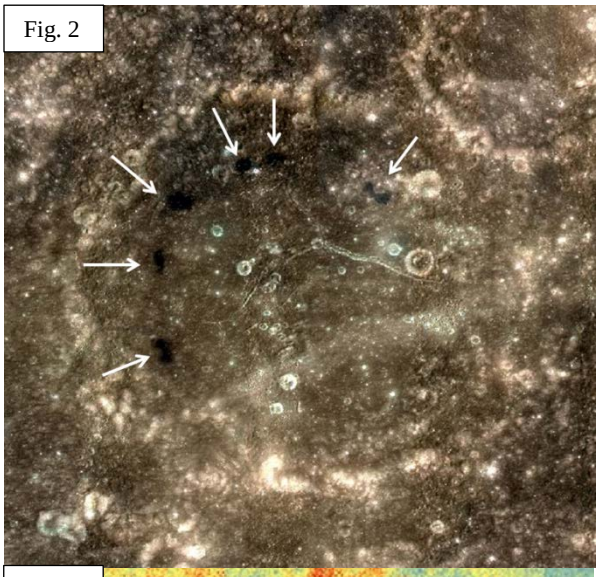

Fig. 3

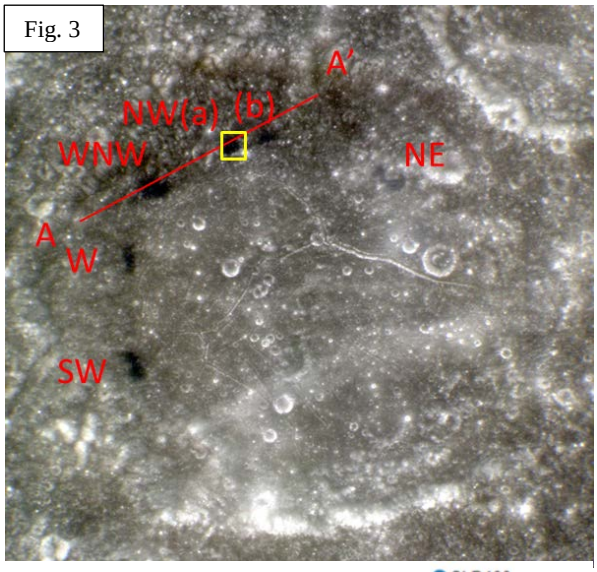

Fig. 4

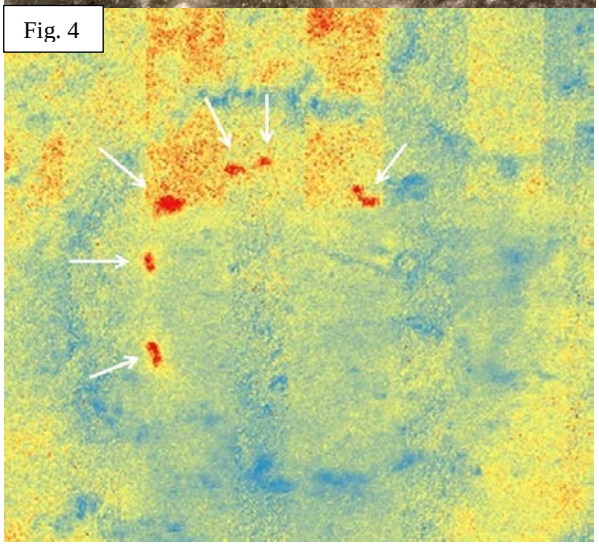

Fig. 5

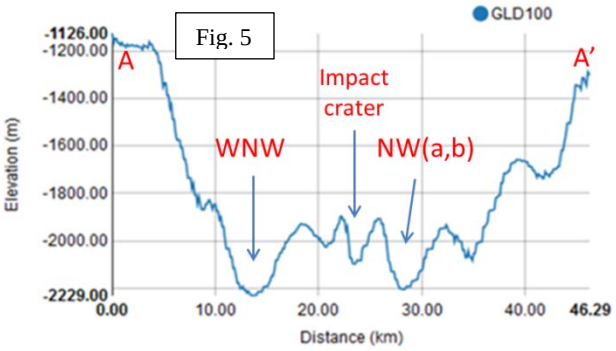

Fig. 6

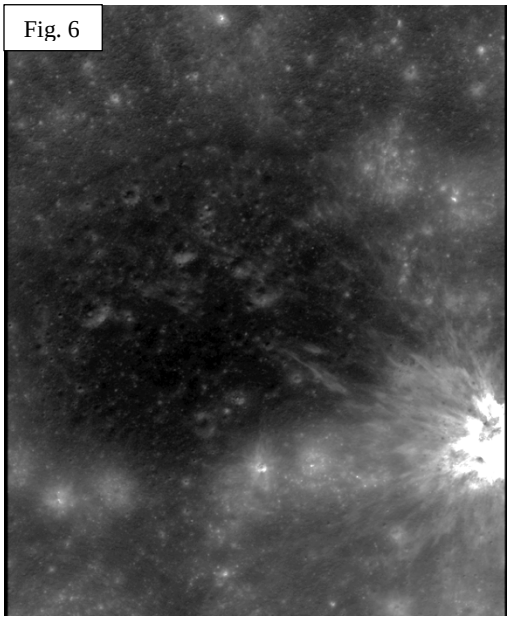

Fig. 6 - Portion of NAC image 1101538799Lshowing the western part of the source crater for the NW deposit (yellow box in Fig. 3). Image width = 3.6 km (NASA/GSFC/ASU).

Fig. 2 - Kaguya MI color image of the Mersenius pyroclastic deposits (arrows). R=900 nm, G=750 nm, B=415 nm. Image width = 100 km. (JAXA)

Fig. 3 - Portion of WAC image M186204976CE showing the same scene. Pyroclastic deposits are labeled according to Coombs & Hawke (1992). Red line A-A' shows the location of the topographic profile in Fig. 5; yellow box shows the location of the NAC image in Fig. 6. R=689 nm, G=604 nm, B=415 nm. (NASA/GSFC/ASU)

Fig. 4 – Kaguya MI derived titanium abundance per Otake *et al.* (2012). Pyroclastic deposits show clearly elevated abundances (warm shades = higher TiO_2). (JAXA)

Fig. 5 – GLD100 topographic profile A-A' as shown in Fig. 3. The WNW and NW source craters have significant topographic expression. (NASA/GSFC/ASU)

References: Coombs & Hawke (1992) *LPS 22nd*, pp 303-312; [2] Hawke *et al.* (2013) *LPS 44th* #1894; [3] Hawke *et al.* (1993) *GRL 20(6)*, 419-422; [4] Robinson *et al.* (2010) *Space Sci. Rev. 150* (1-4), 81-124; [5] Haruyama *et al.* (2008) *Adv. Sp. Res. 42*, 310-316; [6] Ohtake *et al.* (2010) *Space Sci. Rev. 154*, 57-77; [7] Scholten *et al.* (2012) *JGR 117*, E00H17; [8] Otake *et al.* (2012) *LPS 43rd* #1905; [9] Head (1974) *PLSC 5th*, 207-222; [10] Gaddis *et al.* (1985) *Icarus 61*, 461-488; [11] Hawke *et al.* (1989) *LPS 19th*, 255-268; [12] Heiken *et al.* (1974) *GCA 38*, 1703; [13] Delano (1986) *JGR 91*, D201; [14] Hawke *et al.* (1990) *LPS 20th*, 249; [15] Gaddis *et al.* (2003) *Icarus 161*, 262-280; [16] Hawke *et al.* (2009) *LPS 40th* #1146; [17] Schultz (1976) *Moon 15*, 241-273; [18] Joswiak *et al.* (2012) *JGR 117*, E11005.